NASA Technical Memorandum 105366

The Effect of Ion Plated Silver and Sliding Friction on Tensile Stress-Induced Cracking in Aluminum Oxide

Harold E. Sliney and Talivaldis Spalvins
Lewis Research Center
Cleveland, Ohio

Prepared for the
Annual Meeting of the Society of Tribologists and Lubrication Engineers
Philadelphia, Pennsylvania, May 4–7, 1992

NASA

THE EFFECT OF ION PLATED SILVER AND SLIDING FRICTION ON TENSILE STRESS-INDUCED CRACKING IN ALUMINUM OXIDE

Harold E. Sliney and Talivaldis Spalvins
National Aeronautics and Space Administration
Lewis Research Center
Cleveland, Ohio 44135

ABSTRACT

A Hertzian analysis of the effect of sliding friction on contact stresses in alumina is used to predict the critical load for crack generation. The results for uncoated alumina and alumina coated with ion plated silver are compared. Friction coefficient inputs to the analysis are determined experimentally with a scratch test instrument employing a 0.2 mm radius diamond stylus. Series of scratches are made at constant load increments on coated and uncoated flat alumina surfaces. Critical loads for cracking are detected by microscopic examination of cross sections of scratches made at various loads and friction coefficients. Acoustic emission and friction trends are also evaluated as experimental techniques for determining critical loads for cracking. Analytical predictions correlate well with the micrographic evidence and with the lowest load at which AE is detected in multiple scratch tests. Friction/load trends are not good indicators of early crack formation. Lubrication with silver films reduced friction and thereby increased the critical load for crack initiation in agreement with analytical predictions.

NOMENCLATURE

E elastic modulus, GPa

H mean Hertz stress, GPa

R radius of hemispherical contact, m

W_o normal static load, N

W_μ normal load during sliding, N

v Poisson's ratio

μ friction coefficient

σ_o surface static tensile stress, GPa

σ_μ surface tensile stress during sliding, GPa

* superscript denoting critical value for crack initiation

INTRODUCTION

It has been shown by a number of investigators[1-3] that the friction coefficients of unlubricated ceramics are generally high, on the order of 0.5 to 1.0. Wear rates are also higher than might be expected considering the high hardness of many ceramics and the extremely

smooth surfaces to which they can be finished. Ceramics often wear by a microfracture mechanism. The origin of this type of wear is the generation of a crack pattern in the near-surface (surficial) region of the tribological contact. The cracks propagate and intersect at and below the surface to produce loose wear particles. Because ceramics are weak in tension and have very little ductility, the surface cracks are formed by surface tensile stresses. These tensile stresses are a strong function of the tangential friction forces in sliding contacts. Therefore, the high friction coefficients characteristics of ceramics are a primary reason for their high wear during unlubricated sliding. It is to be expected, therefore, that reduction in friction, while desirable in itself, should also alleviate the problem of wear by microfracture.

One way to reduce the friction of ceramics is to coat them with soft, metallic films. Erdemir has shown that ceramics can be coated with adherent, lubricative films of silver by ion beam assisted deposition (IBAD).[4] This is a line-of-sight process that coats only those surfaces that are in the straight line path of the ion beam. The same can be said about other PVD processes such as sputtering although magnetron sputtering has a limited throwing power because of the magnetically curved path of the ion plasma. Ion plating is another PVD process, and it has the advantage of superior "throwing power," or the ability to deposit films around corners and even on the back of specimens. Direct ion plating cannot be done on electrical insulators such as most ceramic materials. However, as reported by the authors in a companion paper,[5] insulators can be coated by placing an accelerating, conductive screen between the filament-heated sources of the coating metal and the ceramic. We call this process screen cage ion plating (SCIP).

In ref. 5, we showed that SCIP-deposited silver reduced the friction coefficients of alumina. In the present paper, we analytically and experimentally determine the effect of this reduced friction on the critical load for producing cracks and microfracture in alumina. The engineering significance of this is to demonstrate the benefits of reduced friction on the dynamic load carrying capacity of ceramic, sliding contact bearing surfaces.

STRESS ANALYSIS

Model

Microstress studies of static and sliding contacts of ceramics have been treated in the literature.[6-8] These analyses clearly demonstrate how sliding friction increases surficial stresses and thereby reduces the critical load, W*, for crack initiation and microfracture damage of brittle materials. Since microfracture is a common wear mode for ceramics, it is of technological interest to quantify the effect of friction coefficient upon the microstresses that are generated in these materials during sliding.

The easiest contact geometry to model for high contact stresses is that of a hemisphere on a flat. A small circular contact area is formed by elastic deformation when a hemisphere is pressed against a flat. For static contacts, the associated stresses are calculated with standard Hertz equations. In our study, the mean static Hertz stress, H_o, and the surface tensile stress component, σ_o, are computed as functions of the normal load on the stylus. Then, the effect of sliding friction on the tensile stress component is calculated. The analyses are discussed in the following section.

Static Hertz Stress

The stresses in the concentrated contact of a sphere against a flat are compressive within the contact circle, but are tensile just outside of the circle. The tensile stress is in the radial direction and is a maximum along the circumference of the contact; it decreases rapidly with distance away from the contact. These compressive and tensile stresses are calculated using the elasticity analysis described in Hertz[9] and in the classic elasticity text by Timoshenko and Goodier.[10] The mean compressive Hertz stress within the static contact of a sphere on flat is given by the equation:

$$H_o = 0.385 \left(\frac{WE^2}{R^2}\right)^{1/3} \tag{1}$$

E is the reduced elastic modulus given by:

$$\frac{1}{E} = \left(\frac{1 - v_1}{E_1}\right) + \left(\frac{1 - v_2}{E_2}\right) \tag{2}$$

where E_1 and E_2 are the elastic moduli of the materials in contact and v_1 and v_2 are the corresponding Poisson's ratios. The values for these properties for diamond and alumina are given in Table I.

The maximum static Hertz stress is 1.5 larger than the mean. The mean is used here for comparison with Vickers indentation hardnesses, which are mean values, and are an upper limit for the valid application of Hertzian elastic analyses.

The scratch test is of course intentionally designed to irreversibly damage (scratch) the surface of the specimen. At the lightest loads, the stylus elastically (reversibly) deforms the surface. As the load is increased, brittle materials such as ceramics crack and fracture. We define the mean Hertz stress at which the first cracks form as the critical mean Hertz stress, H_o^*. The associated critical tensile stress component and load are σ_o^* and W_o^*.

The mean Hertz stress, H_o, for a 0.2 mm radius diamond stylus on alumina was calculated from eqs. (1) and (2) and the elastic properties listed in Table I. Figure 2 gives H_o as a function of normal loads up to 50 N for the static contact of the diamond stylus on alumina. Corresponding curves for 4.76 mm radius diamond and alumina spherical contacts are also given. This larger radius is commonly used in pin on disk friction and wear tests and is included for reference. The calculated H_o is about 18.5 GPa at a stylus load of 50 N. This is above the indentation pressure of 15.7 to 17.7 GPa for alumina derived from published Vickers hardness numbers of 1600 to 1800 kg/mm.[2,14,15] We can expect the critical stress for microcrack initiation to be somewhat lower than the indentation pressure. For example, Ikawa and Shimada reported critical stresses for cracking of sapphire in static contact with a 0.2 mm radius diamond stylus to be about 25 percent lower than the indention hardness.[6] However, in the following discussion, we will take $H_o^* = 17$ GPa for the formation of significant surficial damage. The corresponding W_o^* computed from eq. (1) is 38 N.

Dynamic Surface Stresses During Sliding

During sliding, the tangential friction force greatly increases the tensile stress component σ_μ. As previously stated, it is this tensile stress component that is primarily responsible for cracking in brittle materials. Therefore, the dynamic critical load, W_u^*, to initiate cracking is much lower than the static critical load, W_o^*. The following discussion considers the effect of sliding friction on the dynamic load capacity of polycrystalline alumina.

According to Hertzian theory, the maximum static tensile stress, σ_o, as a function of H_o and Poisson's ratio is expressed by the following equation:

$$\sigma_o = \frac{1}{2}(1 - 2v)H_o \tag{3}$$

For alumina with a Poisson's ratio of 0.23, σ_o is 0.27 H_o and for the assumed H_o^*, of 17 GPa, σ_o is 4.6 GPa. This will be taken as σ_o^* for alumina throughout this paper. We will next consider the effect of friction on the magnitude of the surface tensile stress during sliding, σ_μ.

Enomoto and Tabor (1981)[11] have reported the effect of friction on increasing the tensile stress component during sliding. They quote Hamiliton and Goodman (1966) [12] who showed that the surface tensile stress is increased during sliding by a multiplying factor:

$$(1 + A\mu) \tag{4}$$

where, μ is the friction coefficient and:

$$A = \frac{3\pi\ (4 + v)}{8(1 - 2v)} \tag{5}$$

For alumina, A = 9.2. Therefore,

$$\sigma_\mu(\text{sliding}) = (1 + 9.2\mu)\sigma_o(\text{static}) \tag{6}$$

A plot of the multiplying factor as a function of μ is given in Fig. 3. To avoid crack formation, σ_μ must not exceed the crack critical value of 4.6 GPa. When we substitute this numerical value into eq. (6)

$$\sigma_o = \frac{4.6}{(1 + 9.2\mu)} \tag{7}$$

Therefore, σ_o and the H_o prior to sliding must be less than their critical values in the static case by a factor of $1/(1 + 9.2\mu)$ to avoid cracking when frictional sliding commences. Because the load is proportional to the third power of H, W_μ^* must be reduced by a factor of $(1/1 + 9.2\mu)^3$ relative to the critical static load, W_o^*. Plots of these two factors as a function of

friction coefficient are given in Fig. 4. They give the fractional reduction in load and associated initial Hertz stress necessary to maintain the same surface tensile stress as in a static contact, and are expressed as the normalized Hertz stress, H_μ/H_o, and the normalized load W_μ/W_o.

The average friction coefficient during constant load scratch tests on alumina is 0.18 at loads up to 20 N. For this case, H_μ/H_o and W_μ/W_o are 0.37 and 0.051 respectively. In other words, W^*_μ for a moderate sliding friction coefficient of 0.18 is only about 5 percent of W^*_o.

For silver plated alumina with a typical friction coefficient of 0.10, $W^*_\mu = 14$ percent of W_o. Therefore, ion plated silver should almost triple the allowable load on alumina in sliding contact with diamond. Computed critical loads and stresses for diamond on uncoated and silver coated alumina are summarized in Table III.

For higher friction coefficients of 0.5 to 1.0, which are characteristic of most unlubricated ceramics, the detrimental effect of friction would be more severe than it is for diamond on alumina. For example, at a friction coefficient of 0.6, $W^*_\mu = 0.36$ percent of W^*_o, and at a friction coefficient of 1.0, $W^*_\mu = 0.10$ percent of W^*_o. Therefore, even very lightly loaded contacts on unlubricated ceramics can be expected to produce cracks during sliding. The conclusion is consistent with the microfracture wear mode that is characteristic of unlubricated ceramics, especially in concentrated contacts and on rough surfaces where the stresses on asperities are higher than stresses computed for ideally smooth surfaces.

EXPERIMENTAL SECTION

Material

The alumina is a sintered, polycrystalline grade of alpha-alumina. Density is 3.78 g/cm^3 or about 95 percent of theoretical. The specimens are flat blocks that are surface ground to a finish of 0.25 to 0.38 μm. We measured an average Vickers hardness of 1607 kg/mm^2. Sasaki[14] reports a value of 1800 kg/mm^2. This or somewhat greater variability can be expected from various sources of alumina.

The silver coatings are 1 and 4 μm thick.

The stylus used in the scratch testing has a tip radius of 0.2 mm and a cone angle of 120°.

Procedure

A schematic diagram of the screen cage ion plating process (SCIP) is shown in Fig. 1. The process is described in some detail in ref. 5. Briefly, the specimen is placed in a vacuum chamber where it is surrounded with a 20 mesh silver screen that functions as an electronic grid. A negative potential is applied to the screen. The evaporation source is the anode. Positively charged ions of the evaporated metal, in this case silver, are accelerated to the screen. Most of them pass through the openings in the screen and are deposited in the neutrally charged substrate within the cage. Since the negative field surrounds the substrate, all surfaces become coated. The surface 180° from the silver evaporation source is coated with about one-fourth the coating thickness of the surface facing the source.

A series of scratches are made with a commercial (Revetest) scratch test machine on uncoated and on SCIP silver-coated alumina specimens. Each scratch is 10 mm long and is

made at a velocity of 10 mm/min. The scratches are made with a constant load on the stylus. The lightest constant load is 1.6 N. Loads are then increased in approximately 5 N increments to 50 N. The friction force and acoustic emission are continuously measured as the scratches are made. The specimens are then sectioned in the direction transverse to the scratch direction, mounted, and polished for metallographic examination to determine the critical load, W_{μ}^{*}, for surficial damage.

RESULTS

Photomicroscopy

Alumina.—The microstress calculations predict that alumina should undergo microfracture damage at all but the lighter stylus loads. This is verified by the cross section photomicrographs of the scratches on both uncoated and coated alumina (Figs. 5(a) to (c) and 6) which show the effect of stylus load on surficial damage. The observed damage is described qualitatively in Table II, and is of two types: (1) microfracture of grain boundaries within the Hertzian zone; and (2) radial cracks propagating beyond the Hertzian zone. Both types are illustrated by SEM micrographs in Figs. 7 and 8. The predicted values for the onset of microfracture damage are quantitatively compared to micrographic evidence in Table III.

Photomicrographs (Fig. 5(a)) of scratch cross sections on alumina show microfracture damage in scratches made at 5.5 N, but not at 1.6 N, in good agreement with analytical predictions of $W_{\mu}^{*} = 1.9$ N.

Silver on Alumina.—Silver coatings of 1 and 4 μm thickness were scratched. Some silver remained in scratches made at the highest loads, but the coatings did not reduce surficial damage at stylus loads above 30 N. However, surficial damage was mitigated by the silver coatings at loads below about 30 N.

A typical friction coefficient for the 1 μm coating is 0.08. The predicted W_{μ}^{*} for a friction coefficient of 0.08 is 7.6 N ($H_m{}^{*} = 9.9$ GPa). Figure 5(b) shows no damage at 5.5 N, the onset of microfracture damage at 10.7 N, and progressively greater damage at higher loads. The observed W^{*} between 5.5 and 10.7 N agrees with the predicted value of 7.6 N.

The friction coefficient for the 4 μm coating is typically 0.10. The predicted W_{μ}^{*} is 5.3 N, but no damage is noticed at 10.7 N, and the onset of damage is seen at 14.7 N. Radial crack propagation is first observed at 30.6 N (Fig. 6). The increased protection by the thicker coating despite a slightly higher friction coefficient is probably due to the greater load sharing capability of the thicker film. Therefore our calculations, that only take frictional effects into account, accurately predicted W_{μ}^{*} for uncoated alumina and alumina coated with 1 μm of silver, but the correlation is not as good for the 4 μm coating.

Friction and Acoustic Emission (AE)

Acoustic emission traces and friction traces for uncoated and SCIP silver coated alumina during progressive load scratch tests are shown in Figs. 9(a) and (b). For uncoated alumina, small increases in AE are seen at about 3 N, and a large increase in AE begins at about 6 N. AE for silver coated alumina begins at 9 N and increases with load. The onsets of AE are in fair agreement with the predicted onset of microfracture and microscopy observations. However, the agreement is not as good in all cases. Table III gives the scatter in AE results in repeat

scratch tests. The highest loads for the onset of acoustic emission were much higher than the predicted W_μ^* values. The best agreement is with the lowest observed AE signals. This is consistent with our observations during constant load scratch tests at loads greater than W_μ^* that AE pulses do not always occur at the beginning of a scratch nor continuously during the scratch. There is apparently a statistical distribution in the critical loads at which detectable AE signals occur. The predicted values of W_μ^* are in agreement with the lowest loads at which AE is detected in repeated single pass scratches of the same specimen.

The friction traces on Fig. 9(b) show that friction coefficients, (the slopes of the F_T versus N traces) are the least reliable indicators for the onset of microfracture damage because friction coefficients do not increase until loads well beyond the onset of microfracture are reached. The increases in slope correlate fairly well with the loads at which radial crack propagation becomes significant, but it is uncertain whether this is a cause and effect relationship or a coincidence.

Comparison of Methods

Micrographic cross sections of the scratches gives the most reliable evidence of W_μ^* and the best correlation with stress analysis predictions. The disadvantage is the time and expense involved in the preparation and examination of the specimen mounts.

AE in progressive load tests is a convenient, quick method. It appears to be a reliable technique for determining W_μ^* if enough tests are done to establish the lower end of the statistical distribution of W_μ^* as a function of load. These lower end values correlate reasonably well with prediction and metallographic evidence.

Friction coefficients are the least reliable of the methods used to determine W_μ^*. In some cases, the roughness of the friction force (F_t) traces increase at loads near W_μ^*, but the slopes (friction coefficient, μ) do not show an upward trend until loads are well above W_μ^*. As shown by Spalvins and Sliney in ref. 5., the friction coefficient of silver coated alumina decreases with increasing load, passes through a minimum, then increases as damage to the alumina substrate progresses. Because of this behavior, we were not able to determine W_μ^* from traces of friction force or friction coefficient as a function of stylus load.

SUMMARY AND CONCLUSIONS

Silver films were applied to aluminum oxide by the screen cage ion plating (SCIP) method. Scratches were made with a diamond stylus at normal loads from 1.6 to 50 N on the uncoated and silver coated surfaces to experimentally determine the critical loads for the onset of crack formation in the alumina substrate. Experimental results were compared with the predictions of surface stress analyses. The major conclusions from this study are:

1. SCIP coated silver reduces the friction of diamond on alumina and thereby increases W_μ^*, the critical load for the onset of microfracture in alumina.

2. The validity of the analytical model to predict the effect of sliding friction on W_μ^* was verified by micrographs of the scratch cross sections made at loads below and above the predicted values of W_μ^*.

3. Acoustic emissions can be used to detect cracking in the alumina as the load is increased. However, in repeated tests, there is considerable data scatter in the load at which the first AE signal is detected. The lowest values in the AE scatter distribution agree with micrographic evidence and analyses.

4. Friction measurements are not useful for detecting early crack generation. Friction coefficients do not generally increase until considerable substrate breakup has occurred.

REFERENCES

1. Sutor, P., "Tribology of Silicon Nitride and Silicon on Nitride-Steel Sliding Pairs," Ceram. Eng. Sci. Proc., **5**, pp. 460-469 (1984).

2. Sikra, J.S., Krysiak, J.E., Eklund, P.R., and Ruh, R., "Friction and Wear Characteristics of Selected Ceramics," Am. Ceram. Soc. Bull., **53**, pp. 581-582 (1974).

3. Breznik, J., Breval, E., and MacMillan, N.H., "Sliding Friction and Wear of Structural Ceramics," J. Mater. Sci., **20**, pp. 4657-4680 (1985).

4. Erdemir, A. et. al., "Solid Lubrication of Ceramic Surfaces by IBAD-Silver Coatings for Heat Engine Applications," Tribol. Trans., **33**, pp. 511-518, (1990).

5. Spalvins, T., Sliney, H.E. and Deadmore, D., "Screen Cage Ion Plating (SCIP) and Scratch Testing of Polycrystalline Aluminum Oxide," NASA TM, 1992. (to be published)

6. Ikawa, N. and Shimada, S., "Microstrength Measurement of Brittle Materials, " Technology Reports of Osaka University, **31**, (1622), pp. 315-323 (1982).

7. Richardson, D.W., Lindberg, J.L., Carruthers, W.D., and Dahn, J., "Contact Stress Effects in Si_3N_4 and SiC Interfaces," Ceram. Eng. Sci. Proc., **2**, pp. 578-588 (1981).

8. Swain, M.V., "Microfracture about Scratches in Brittle Solids." Proc. Roy. Soc. London, Ser. A, **366**, pp. 575-597 (1979).

9. Hertz, H., "On the Contact of Elastic Solids," J. Math. (Crelle's Jour.), **92.** pp. 156-171 (1881).

10. Timoshenko, S. and Goodier, J.N., Theory of Elasticity, 2nd edition, McGraw-Hill, (1951).

11. Enomoto, Y. and Tabor, D. "The Frictional Anisotropy of Diamond," Proc. Roy. Soc. London, Ser. A, **373**, pp. 405-417 (1981).

12. Hamilton, G.M. and Goodman, L.E., "The Stress Field Created by a Circular Sliding Contact," J. Appl. Mech., **33**, pp. 371-376 (1966).

13. Chrenko, R.M. and Strong, H.M., "Physical Properties of Diamond," General Electric R&D Rept. GIDEP-E062-0548 (1975). (Avail. NTIS, AD-B035657L).

14. Sasaki, S., "The Effects of Surrounding Atmosphere on the Friction and Wear of Alumina, Zirconia, Silicon Carbide, and Silicon Nitride," Wear of Materials, Vol. 1, ASME, pp. 409-417 (1989).

15. Sliney, H.E. and Deadmore, D.L., "Friction and Wear of Oxide Ceramic Sliding Against IN-718. Nickel Base Alloy at 25 to 800 °C in Atmospheric Air," NASA TM-102291 (1989).

TABLE I.—ELASTIC PROPERTIES AND HARDNESS OF DIAMOND AND ALUMINA

	Elastic modulus		Poisson's ratio	Vicker's hardness	
	GPa	PSI/10^6	------	GPa	kg/mm^2
Diamond	[a]1020	148	[b]0.20	[a]88	8333
Alumina	[c]363	53	[c]0.23	18	[c]1800 [d]1600

[a]Ikawa and Shimada (1981).[6]
[b]Chrenko and Strong (1975).[13]
[c]Saski, S. (1989).[14]
[d]Measured in authors' laboratory.[15]

TABLE II.—QUALITATIVE OBSERVATIONS OF SCRATCH CROSS SECTIONS BY OPTICAL MICROSCOPY AT X200

[Legend: C: Propagated cracks, D: Grain boundary damage.]

Nominal load, N	Uncoated alumina	1 μm Ag/alumina	4 μm Ag/alumina
1.6	No damage	No damage	No damage
5.0	Slight D	No damage	No damage
10	Slight D	Slight D	No damage
15	Moderate D	Slight D	Slight D
20	One C, mod. D	Moderate D	Moderate D
25	Moderate C, D	Moderate D	Moderate D
30	Increased C & D	One C, mod. D	One C, mod. D
35	Severe C & D	Increased C & D	Increased C & D
40	Severe C & D	Severe C & D	Severe C & D
50	Severe C & D	Severe C & D	Severe C & D

TABLE III.—CALCULATED AND OBSERVED CRITICAL STYLUS LOADS FOR 0.2 mm RADIUS DIAMOND ON ALUMINA

Silver coating thickness, μm	Friction coefficient, μ	Calculated		Critical Load W*			
		Critical mean Hertz stress H*, GPa	Critical load W*, N	Experimental			
				Micrographic, N	Acoustic emission		
					Number of tests	Scatter, N	Average, N
None (Static)	0	17	38	----------	5	36-52	42
None	.18	6.3	1.9	1.6 > 5.5	8	2-9	4.5
1	.08	9.9	7.6	5.5 > 10.7	6	6-10	7.8
4	.10	8.8	5.3	10.7 > 14.7	7	5-17	9.3

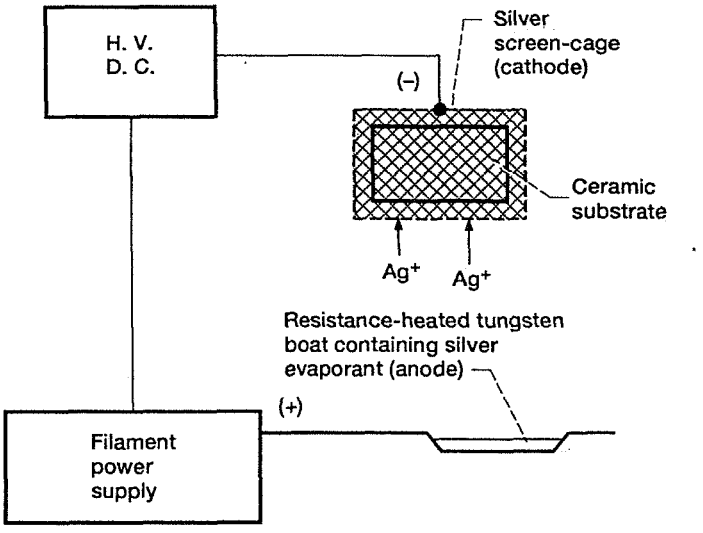

Figure 1.—Schematic for screen-cage ion plating of ceramics.

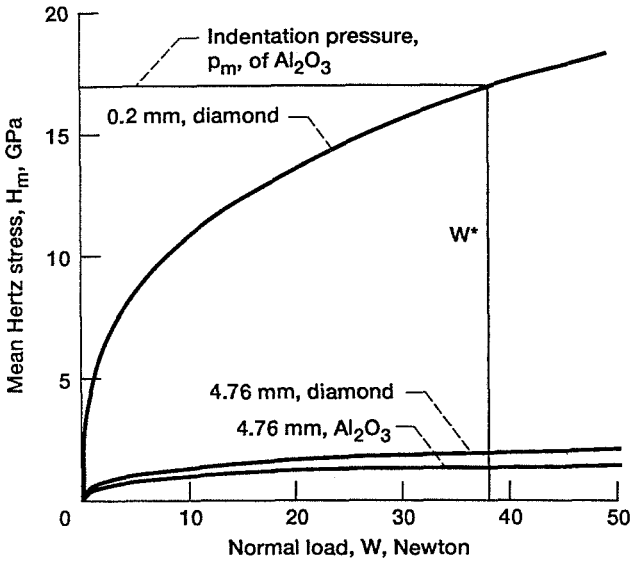

(a) Linear scale.

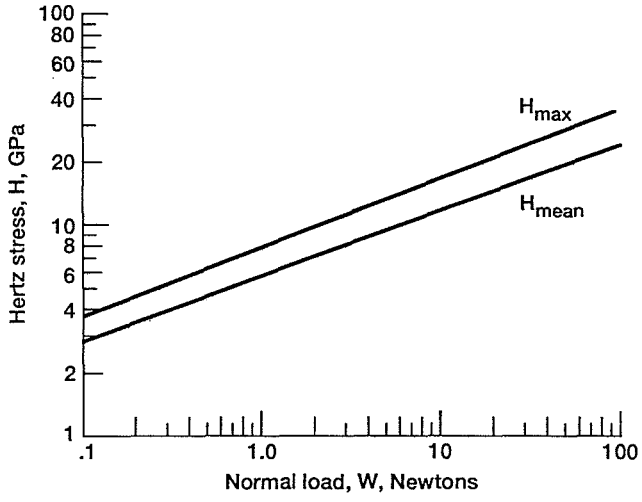

(b) Log-log scale.

Figure 2.—Mean Hertz stress; (a) H_m for static contact of 200 μm and 4.76 mm radii diamond and for 4.76 mm radius aluminum oxide hemispheres on polycrystalline aluminum oxide flat and (b) H_{max} and H_m for 200 μm diamond on aluminum oxide.

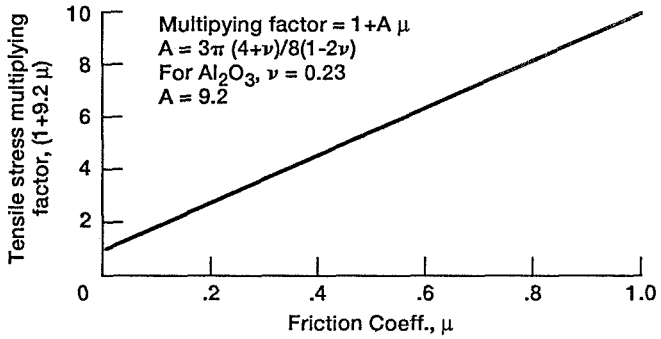

Figure 3.—Effect of dynamic friction coefficient on the tensile stress component in a ball on flat hertzian contact on alumimum oxide.

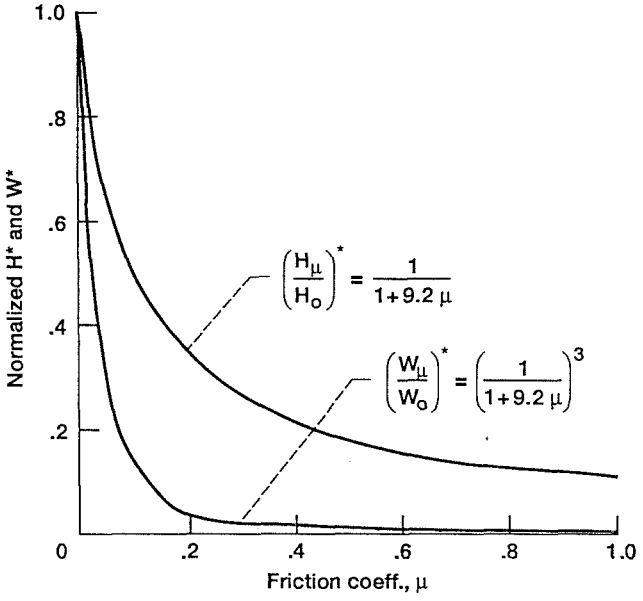

Figure 4.—The effect of friction coefficient on reducing the critical load, W*, and initial hertz stress, H^*_o, to produce tensile cracks during sliding of a hemisphere on an alumina flat.

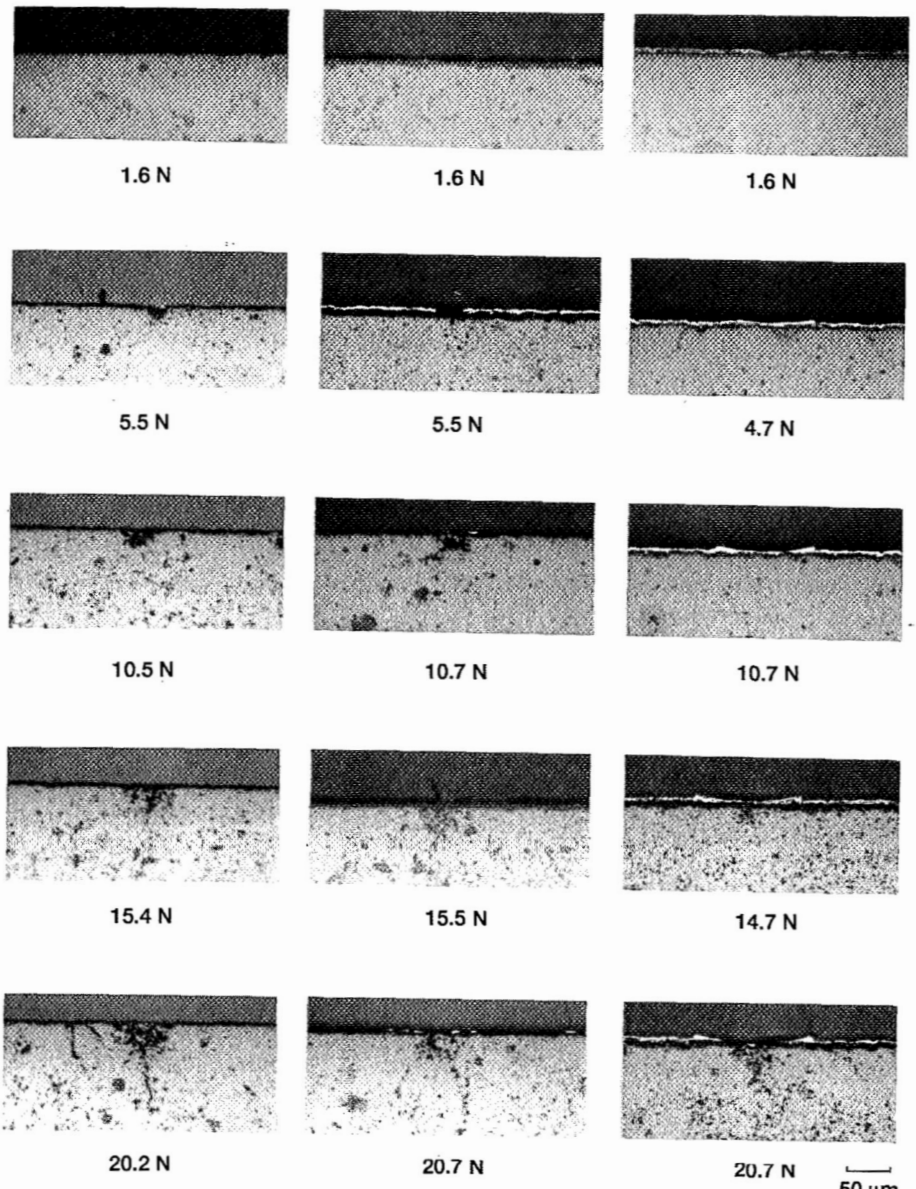

Figure 5.—Progressive microfracture with increasing load.

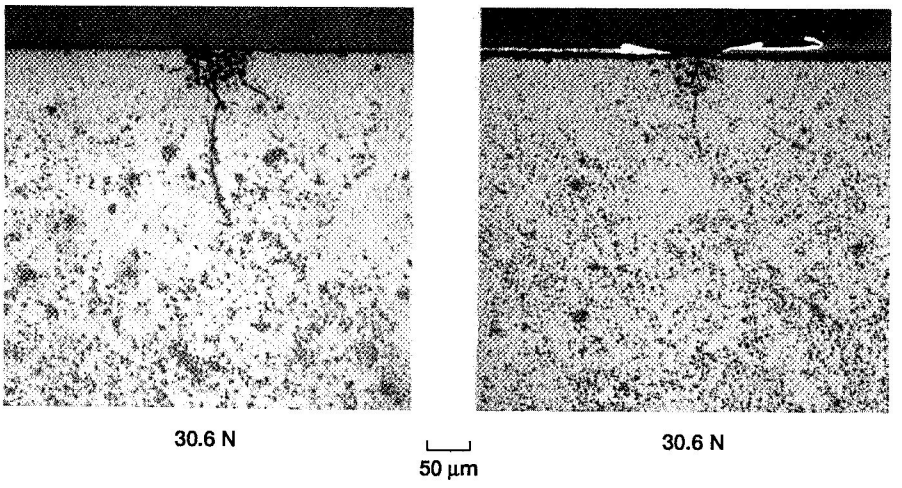

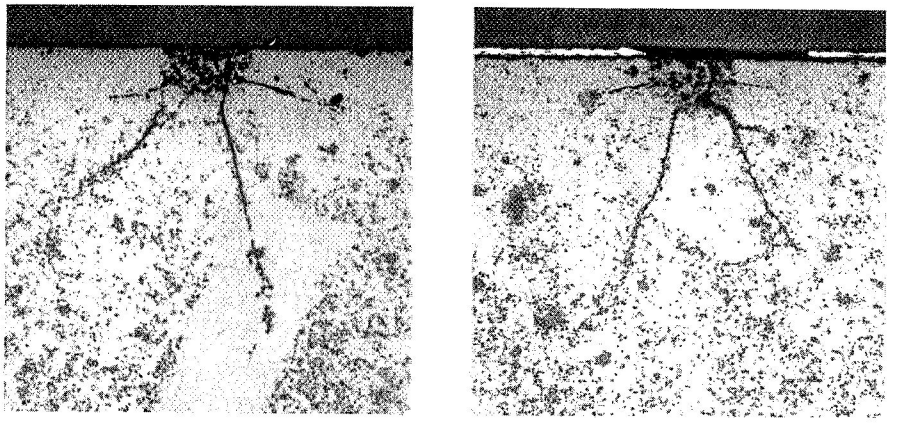

Uncoated alumina

4 μm Silver on alumina

Figure 6.—Progressive microfracture and radial crack propagation at high loads.

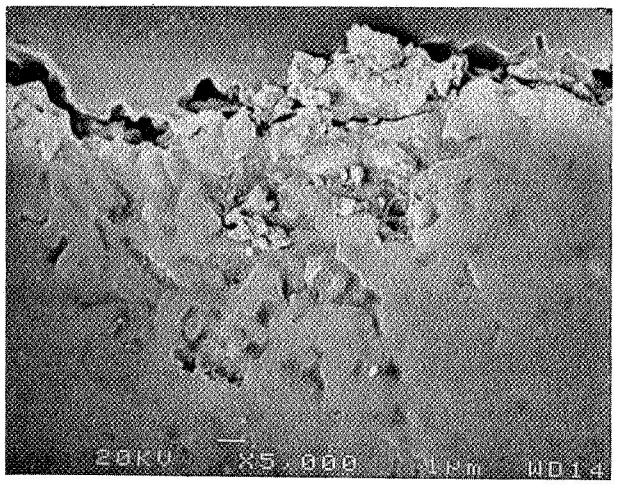

Figure 7.—SEM micrograph of microfracture damage in the hertzian zone under a scratch made on alumina at a 5.5 N stylus load.

ORIGINAL PAGE
BLACK AND WHITE PHOTOGRAPH

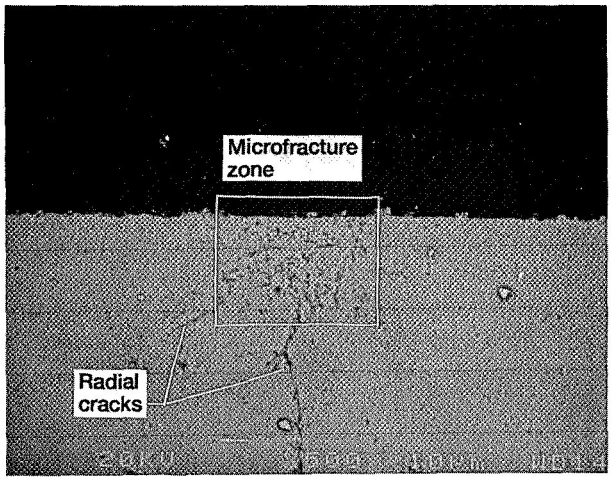

(a) Microfracture and radial crack damage.

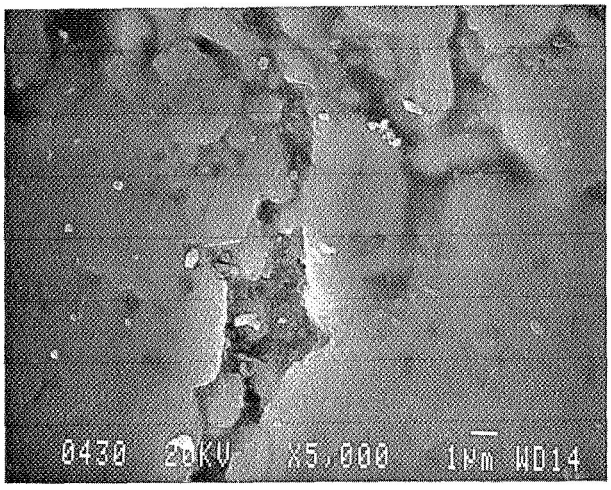

(b) Radial crack initiation and propagation site.

Figure 8.—SEM micrographs of severe damage under a scratch made on alumina at a 30.5 N stylus load.

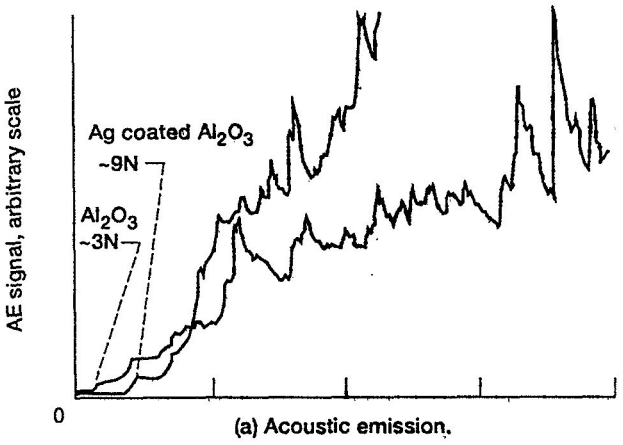

(a) Acoustic emission.

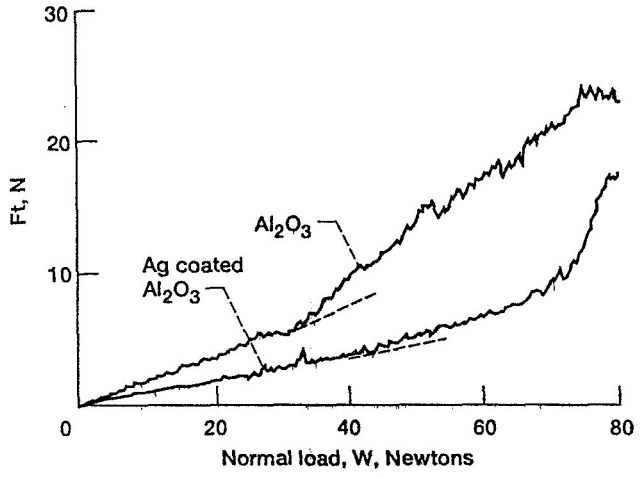

(b) Friction.

Figure 9.—Effect of "SCIP" silver coating in scratch tests of alumina.

REPORT DOCUMENTATION PAGE

Form Approved
OMB No. 0704-0188

1. AGENCY USE ONLY (*Leave blank*)	2. REPORT DATE	3. REPORT TYPE AND DATES COVERED
	1991	Technical Memorandum

4. TITLE AND SUBTITLE

The Effect of Ion Plated Silver and Sliding Friction on Tensile Stress-Induced Cracking in Aluminum Oxide

5. FUNDING NUMBERS

WU-505-63-5A

6. AUTHOR(S)

Harold E. Sliney and Talivaldis Spalvins

7. PERFORMING ORGANIZATION NAME(S) AND ADDRESS(ES)

National Aeronautics and Space Administration
Lewis Research Center
Cleveland, Ohio 44135-3191

8. PERFORMING ORGANIZATION REPORT NUMBER

E-6651

9. SPONSORING/MONITORING AGENCY NAMES(S) AND ADDRESS(ES)

National Aeronautics and Space Administration
Washington, D.C. 20546-0001

10. SPONSORING/MONITORING AGENCY REPORT NUMBER

NASA TM-105366

11. SUPPLEMENTARY NOTES

Prepared for the Annual Meeting of the Society of Tribologists and Lubrication Engineers, Philadelphia, Pennsylvania, May 4-7, 1992. Responsible person, Harold E. Sliney, (216) 433-6055.

12a. DISTRIBUTION/AVAILABILITY STATEMENT

Unclassified - Unlimited
Subject Category 27

12b. DISTRIBUTION CODE

13. ABSTRACT (*Maximum 200 words*)

A Hertzian analysis of the effect of sliding friction on contact stresses in alumina is used to predict the critical load for crack generation. The results for uncoated alumina and alumina coated with ion plated silver are compared. Friction coefficient inputs to the analysis are determined experimentally with a scratch test instrument employing a 0.2 mm radius diamond stylus. Series of scratches are made at constant load increments on coated and uncoated flat alumina surfaces. Critical loads for cracking are detected by microscopic examination of cross sections of scratches made at various loads and friction coefficients. Acoustic emission and friction trends are also evaluated as experimental techniques for determining critical loads for cracking. Analytical predictions correlate well with the micrographic evidence and with the lowest load at which AE is detected in multiple scratch tests. Friction/load trends are not good indicators of early crack formation. Lubrication with silver films reduced friction and thereby increased the critical load for crack initiation in agreement with analytical predictions.

14. SUBJECT TERMS

Ceramics; Surface stresses; Indentation stress; Friction stress; Ion plating of ceramics

15. NUMBER OF PAGES

16

16. PRICE CODE

A03

17. SECURITY CLASSIFICATION OF REPORT	18. SECURITY CLASSIFICATION OF THIS PAGE	19. SECURITY CLASSIFICATION OF ABSTRACT	20. LIMITATION OF ABSTRACT
Unclassified	Unclassified	Unclassified	